Origin of coupling to antisymmetric modes in arc-induced long-period fiber gratings

O. V. Ivanov[1*] and G. Rego[2, 3]

[1]*Ulyanovsk Branch of Institute of Radio Engineering and Electronics of Russian Academy of Sciences, ul. Goncharova 48, Ulyanovsk 432011, Russia*
[2]*INESC Porto, Unidade de Optoelectrónica e Sistemas Electrónicos, Rua do Campo Alegre 687, 4169-007 Porto, Portugal*
[3]*Escola Superior de Tecnologia e Gestão, Instituto Politécnico de Viana de Castelo, Av. do Atlântico, Apartado 574, 4901-908 Viana do Castelo, Portugal*
**Corresponding author: olegivvit@yandex.ru*

Abstract: We study the origin of antisymmetric perturbation of the fiber in arc-induced long-period gratings that couple the core mode into the antisymmetric cladding modes. We demonstrate that this perturbation is caused by the temperature gradient in the fiber, which is induced, in turn, by the temperature gradient in the arc discharge. The reproducibility of the process of the grating inscription is higher when the fiber is placed in a region with larger temperature gradient.

OCIS codes: (060.2340) Fiber optics components; (050.2770) Gratings

References and links

1. G. Rego, R. Falate, J. L. Fabris, J. L. Santos, H. M. Salgado, S. L. Semjonov, and E. M. Dianov, "Arc-induced long-period gratings in aluminosilicate glass fibers," Opt. Lett. **30**, 2065-2067 (2005).
2. G. Rego, A. Fernandez Fernandez, A. Gusarov, B. Brichard, F. Berghmans, J. L. Santos, and H. M. Salgado, "Effect of ionizing radiation on the properties of long-period fiber gratings," Appl. Opt. **44**, 6258-6263 (2005).
3. G. Rego, R. Falate, O. Ivanov, and J. L. Santos, "Simultaneous temperature and strain measurements performed by a step-changed arc-induced long-period fiber grating," Appl. Opt. **46**, 1392-1396 (2007).
4. G. Rego, O. Ivanov, and P. V. S. Marques, "Demonstration of coupling to symmetric and antisymmetric cladding modes in arc-induced long-period fiber gratings," Opt. Express **14**, 9594-9599 (2006).
5. L. Xiao, W. Jin, M. S. Demokan, H. L. Ho, Y. L. Hoo, and C. Zhao, "Fabrication of selective injection microstructured optical fibers with a conventional fusion splicer," Opt. Express **13**, 9014-9022 (2005).
6. M. Tachikura, "Fusion mass-splicing for optical fibers using electric discharges between two pairs of electrodes," Appl. Opt. **23**, 492-498 (1984).
7. F. Durr, G. Rego, P. V. S. Marques, S. L. Semjonov, E. Dianov, H. G. Limberger, and R. P. Salathé, "Stress profiling of arc-induced long period fiber gratings," J. Lightwave Technol. **23**, 3947-3953 (2005).
8. R. H. Doremus, "Viscosity of silica," J. Appl. Phys. **92**, 7619-7629 (2002).
9. G. Rego, L. M. N. B. F. Santos, B. Schröder, P. V. S. Marques, J. L. Santos, and H. M. Salgado, "In situ temperature measurement of an optical fiber submitted to electric arc discharges," IEEE Photon. Technol. Lett. **16**, 2111-2113 (2004).
10. G. Rego, O. Ivanov, P. V. S. Marques, and J. L. Santos, "Investigation of formation mechanisms of arc-induced long-period fiber gratings," in Proc. of OFS-18, paper TuE84 (2006).
11. S. A. Vasiliev and O. I. Medvedkov, "Long-period refractive index fiber gratings: properties, applications, and fabrication techniques," Proc. SPIE **4083,** 212-223 (2000).

1. Introduction

Long-period fiber gratings (LPFGs) fabricated by the electric arc technique demonstrate some specific properties that make them promising for applications in sensing and optical communications [1–3]. In particular, these LPFGs have high temperature stability, exhibit good resistance to gamma radiation, and enable flexible tuning of their sensitivity to changes in physical parameters such as temperature and strain. The arc-induced LPFGs have been studied for quite a long-time; however, the mechanism of grating formation is still not well understood and there is a problem of reproducibility. As we have demonstrated recently, cladding modes of different symmetries are excited by LPFGs inscribed in different fibers by the same technique [4]. Therefore, different mechanisms are involved in the formation of arc-

#83839 - $15.00 USD Received 7 Jun 2007; revised 13 Aug 2007; accepted 13 Aug 2007; published 8 Oct 2007

induced gratings. Among those mechanisms may be modulation of core diameter due to fiber tapering, strain induction or relaxation, microbending and microdeformation.

The LPFGs arc-induced in SMF-28 fiber using the setup described in [1] couple the core mode to the LP_{1i} cladding modes, the corresponding perturbation being antisymmetric. The origin of this asymmetry in the perturbation is unknown. In this paper, we investigate the process of grating inscription in more detail to find the asymmetric factor. In particular, we measure the temperature gradient in the arc and the resulting temperature gradient in the fiber. We discuss the contribution of the latter gradient to the formation of LPFGs in SMF-28 fiber. One of the consequences of the temperature gradient is the periodical microdeformation that consists in a shift of the fiber core under arc discharges. We analyze if such microdeformation can be responsible for the coupling to the antisymmetric cladding modes.

2. Temperature distribution in the arc discharge

The arc-induced LPFGs are created in an optical fiber through a periodical exposure along its length to arc discharges produced by a fusion splicing machine. During the writing process, the fiber is kept under longitudinal tension, which thins and elongates the fiber section heated by the arc. Normally, the fiber is placed in the center between the electrodes. This position is the center of symmetry of the setup, and therefore it was earlier assumed that this is the optimum position, the temperature being highest and the temperature gradient being smallest here [5, 6]. However, the analysis of the symmetry of cladding modes excited by the LPFGs written with the use of our setup in SMF-28 fiber has revealed that the perturbation induced in these gratings is antisymmetric. We also note that the tomographic stress profiles of the fiber regions submitted to the arc discharge exhibit asymmetry [7].

In order to understand the origin of asymmetry of this perturbation, we study the temperature distribution in the arc that is applied to the fiber. In our setup, the current in the arc is direct (dc). Therefore, the arc is directional and the center between the electrodes is not the center of symmetry. This can be seen in the photograph of the arc discharge in Fig. 1. The electrode at the bottom (cathode) glows only at its tip, while the electrode at the top (anode) glows over a much larger area. The arc itself is brighter near the lower electrode. Thus, we expect that there is a gradient of temperature circularly symmetric with respect to the line joining the electrodes (the *y* axis).

To estimate the temperature gradient in the arc, we measured the dependence of the fiber diameter reduction, in the section heated by the arc, on the position of the fiber with respect to the electrodes (in the *y*–*z* plane). The decrease in the fiber diameter is a function of fluidity of the fiber in the arc and the duration of the arc or, rather, a function of the product of the fiber fluidity (which is assumed to be constant over the cross-section of the fiber) and the arc duration: $\Delta D = K(tF)$. This function can be obtained by measuring the decrease in the fiber diameter for various values of the arc duration or, equivalently, by applying the same discharge (having duration t_0) several times (N times) on the same fiber section:

$$\Delta D = K(Nt_0F_0) = G(N). \qquad (1)$$

F_0 is the fiber fluidity in the arc and is constant for all discharges. Knowing the function G, we can calculate the fiber fluidity in a different arc from the decrease in diameter upon one discharge as $F = F_0 G^{-1}(\Delta D)$, where G^{-1} is the inverse of the function G.

The dependence of the fiber diameter reduction on the number of discharges is shown in Fig. 2. We fitted the inverse of this dependence by a polynomial curve of the third order. The formula shown in this figure is exactly the expression for the function $G^{-1}(\Delta D)$. Then we placed the fiber in the *x*–*y* plane and measured the dependence of the fiber diameter reduction on the *y* coordinate. Using the expression for G^{-1}, we obtained the fiber fluidity normalized by F_0, which is shown in Fig. 3 by the dashed curve. Afterwards, the temperature was calculated by using the following equation (derived from the dependence of the silica viscosity on temperature in the range 1000–1400 ºC; Eq. (2) from Ref. [8]):

#83839 - $15.00 USD Received 7 Jun 2007; revised 13 Aug 2007; accepted 13 Aug 2007; published 8 Oct 2007

$$\log F = 12.4 - \frac{37192}{T}, \qquad (2)$$

where F is the silica fluidity ($Pa^{-1}s^{-1}$) and T is the temperature (K). The temperature gradient is shown by the solid curve of Fig. 3. To find the absolute value of F we used F_0, which was obtained by assuming that the temperature of the fiber in the center between the electrodes is 1350 ºC [9]. Similar measurements were made with the fiber shifted along the z axis. In Fig. 4, the corresponding fluidity and temperature gradients are shown. From Figs. 3 and 4, we obtained a constant temperature gradient of ~0.35 ºC/μm along the y axis and a temperature gradient having a maximum of ~0.7 ºC/μm along the z axis.

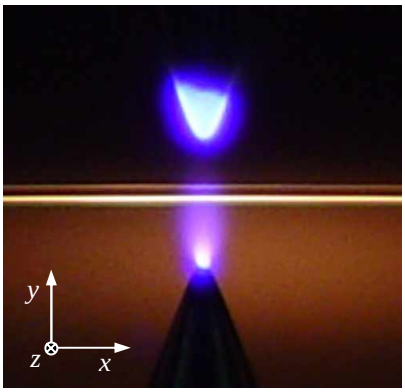

Fig. 1. Photograph of the arc discharge showing its asymmetry.

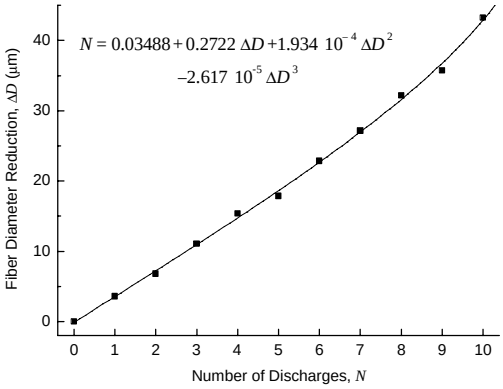

Fig. 2. Fiber diameter reduction versus the number of discharges.

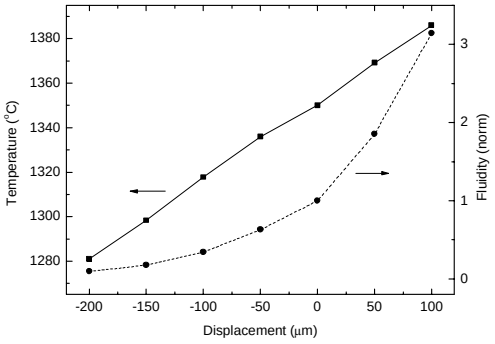

Fig. 3. Fiber temperature and fluidity along the y axis.

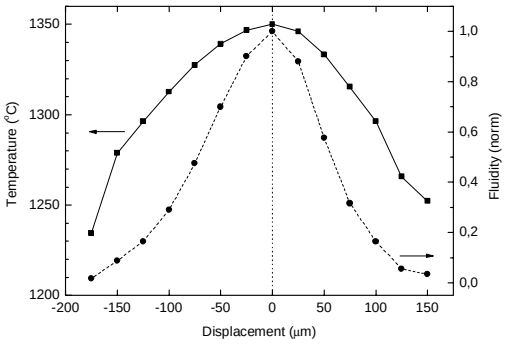

Fig. 4. Fiber temperature and fluidity along the z axis.

3. Asymmetry of perturbation in the fiber

As we have shown in the previous section, wherever in the arc the fiber is positioned, there is always a temperature gradient. This gradient is quite high: when the fiber is shifted along the y axis by the distance equal to its diameter (125 μm), the fiber fluidity changes by a factor of 4–5; the change may be even higher when the fiber is shifted along the z axis. This is demonstrated in Fig. 5, which shows the fluidity ratio between the two sides of the fiber in the arc, neglecting the thermal conductivity of the silica. The value of this ratio was calculated from the temperature difference between two points separated by 125 μm. If the fiber is in the center between the electrodes, only the temperature gradient in the y direction is present. However, an error, for example, of 20 μm in the z coordinate of the fiber produces such a

#83839 - $15.00 USD Received 7 Jun 2007; revised 13 Aug 2007; accepted 13 Aug 2007; published 8 Oct 2007

temperature gradient that the fiber fluidity differs by a factor of 2 in two points separated by 125 μm. We should expect that the temperature gradient in the arc can create some temperature gradient inside the fiber itself, the latter gradient being weaker due to thermal conductivity of the fiber. Therefore, we attempted to reveal the existence of a temperature gradient inside the fiber, which may be the asymmetric perturbation that forms the LPFG.

Two types of geometric deformation of the fiber occur in an arc discharge: tapering and microbending. Tapering is a symmetric diameter reduction and an elongation of the fiber. The degree of tapering of the fiber depends on the pulling tension and also on the value and duration of the electric current in the arc. With typical arc discharge parameters (current of 9 mA and duration 1 s), diameter reductions of ~5% and ~10% were obtained for tensions of 22.8 g and 36.3 g, respectively. For a tension of 5.1 g, the reduction is below 1%. This fiber deformation induces coupling to symmetric modes. However, as we have shown recently [10], the coupling constant corresponding to a typical fiber diameter reduction of a few percent is too small to explain the grating formation. The microbending occurs when the fiber body is locally displaced in the plane lateral to the fiber axis due to some asymmetry in the setup.

We scrutinized the sections of fibers exposed to the arc and found an asymmetry in their deformation. Figure 6(a) shows a photograph (squeezed in the longitudinal direction) of a SMF-28 fiber with a diameter modulation of ~5% obtained during inscription of a 540-μm grating, where the modulation on the left side is visibly larger than on the right side. Figure 6(b) illustrates how such a difference between the two sides of the fiber induces a core shift or geometrical microbending that may lead to the grating formation. The core follows the medial line between the right and left sides of the fiber. This line is not straight due to the difference between the right and left side modulations. We believe that the difference between the deformations on the opposite sides is caused by the difference in viscosity of silica. This difference in viscosity itself is due to the temperature difference.

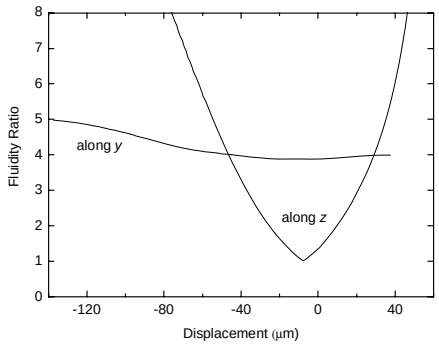

Fig. 5. Fluidity ratio between two sides of the fiber along the *y* and *z* axes.

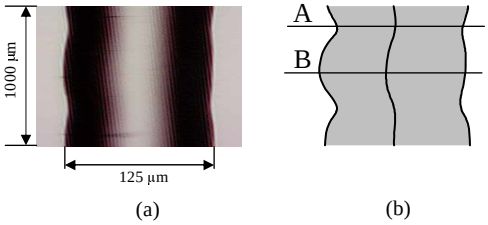

Fig. 6. (a). Photograph of a fiber modified by arc discharges; (b) shift of the fiber central line.

To estimate the viscosity difference between the two sides of the fiber heated by the arc, we could measure the corresponding deformations. However, the deformations being small, this measurement is difficult to carry out. Therefore, we placed a silica capillary into the arc instead of the fiber and pressurized it. The capillary was asymmetrically swollen (Fig. 7). The increase in diameter is approximately proportional to the silica fluidity at a particular point. From a dozen of swollen capillaries having various diameters of the swell, we found that the difference in fluidity between the opposite sides of the capillary is a factor of 1.5–2, which corresponds to a temperature difference of about 20 °C. This is less than in Fig. 5, which agrees with our reasoning.

#83839 - $15.00 USD Received 7 Jun 2007; revised 13 Aug 2007; accepted 13 Aug 2007; published 8 Oct 2007

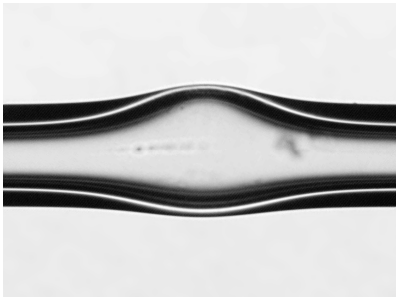

Fig. 7. Asymmetric deformation of a silica capillary (56/125 μm) submitted to an arc-discharge.

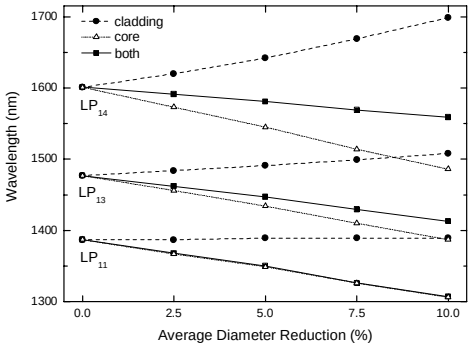

Fig. 8. Resonance wavelengths as a function of the geometric modulation.

As we mentioned above, the symmetric tapering of the fiber cannot induce coupling to the antisymmetric cladding modes; however, it has an influence on the spectra of LPFGs, because the average fiber diameter decreases and causes a wavelength shift of the LPFG resonances (Fig. 8). As seen from the figure, while the reduction of the cladding diameter leads to increases in the resonance wavelengths, the reduction of the core diameter leads to opposite changes. The figure also shows that the effect of the core thinning for the first asymmetric cladding modes is predominant when both the core and cladding are reduced simultaneously.

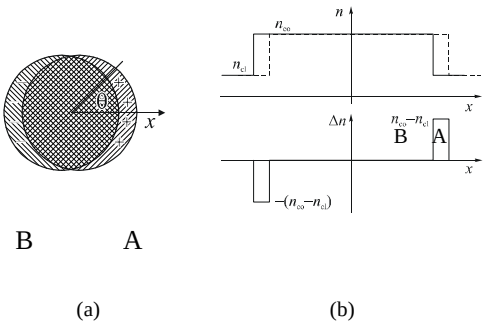

Fig. 9. (a). Refractive index change due to the shift of the fiber core; (b) refractive index change along the *x* axis.

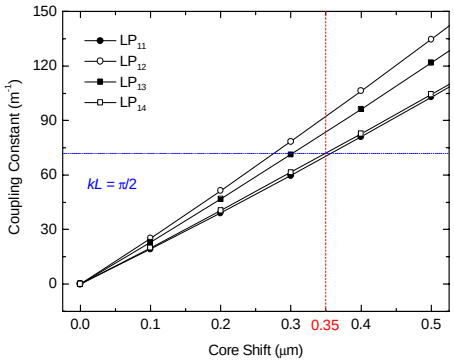

Fig. 10. Coupling constant as a function of the core shift.

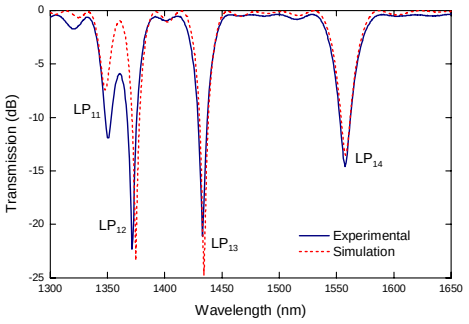

Fig. 11. Transmission spectrum of an LPFG: experimental (solid line) and simulation (dashed line).

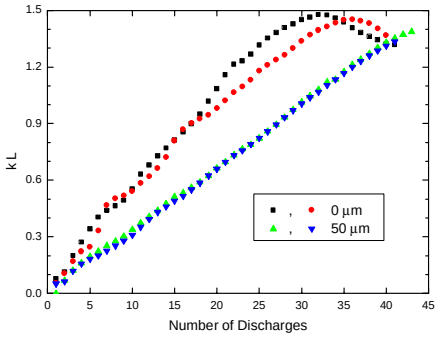

Fig. 12. Normalized coupling constant for the 4-th cladding mode of LPFGs written at two positions.

#83839 - $15.00 USD Received 7 Jun 2007; revised 13 Aug 2007; accepted 13 Aug 2007; published 8 Oct 2007

The periodical core shift couples the core mode to the antisymmetric LP_{1j} modes. To determine the influence of the value of the core shift on the coupling strength we use the coupled mode theory. The coupling coefficient is defined through the overlap integral between the core and cladding mode fields and the perturbation Δn induced by the core shift and can be expressed as $C\pi\Delta n I/\lambda_r$, where I is the overlap integral, λ_r is the resonance wavelength, and C is the constant equal to the first coefficient in the Fourier transform of the grating pitch shape [11]. There are only two regions where the perturbation is nonzero: one of them is near the core radius and the other is near the cladding radius. Figures 9(a) and 9(b) show the refractive index change in this fiber ($\Delta n = 0.0052$, D_{co}=8.2 μm). Δn is equal to $n_{co} - n_{cl}$ at around r_{co} and $n_{cl} - 1$ at around r_{cl}. The change at the cladding–air interface can be neglected in the calculation of the coupling coefficient because the core mode amplitude is vanishingly small at this interface. Using the perturbation that is shown in Fig. 9, we calculated the coupling constant as a function of the core shift for the first four cladding modes (Fig. 10). As seen from Fig. 10, the coupling coefficient increases with an increase in the core shift achieving 100% coupling ($kL = \pi/2$) for values in the range 0.3–0.35 μm. The value of the core shift measured from Fig. 6 is of about 0.35 μm, being, therefore, sufficient to obtain gratings with large coupling strength. Assuming the value of the core shift to be 0.35 μm, we fitted the experimental spectrum of an arc induced LPFG with a length of 21.6 mm by using the simulation program Apollo v2.2 (Fig. 11). It is seen that the simulation agrees well with the experiment.

As we mentioned in the introduction, there is a problem of reproducibility for the arc-induced LPFGs. Normally, the fiber during the inscription process is positioned on the line between the electrodes. Therefore, the temperature gradient along the *z* axis should be zero in this case. However, a small uncontrolled displacement of about 20 μm in the *z* coordinate may change this gradient from zero to a large magnitude. We suppose this is why the reproducibility of the inscription is usually low. To improve the situation, it is possible to shift the fiber from the center position to one or another side. This would make the gradient in the *z* direction nonzero and its value would not depend so strongly on the fiber position. To examine our hypothesis we investigated the reproducibility of the technique in two different positions of the fiber. We followed the growth of gratings (SMF28, 13 g, 9 mA, 1s, 540 μm), discharge by discharge (the transmission loss of LP_{14} was monitored), for two different positions along the z axis: 0 and 50 μm. We also shifted the fiber by 100 μm closer to the colder electrode, where the arc is wider. Two gratings were written in each position. It was observed that, for the fiber displaced by 50 μm from the line between the electrodes, the growth of the resonance is smooth and linear and the two curves corresponding to the same writing parameters almost coincide (Fig. 12). Whereas, for the fiber without displacement, the growth is not so linear and the two curves diverge significantly. This demonstrates higher reproducibility in the case when the fiber is displaced. For the same number of discharges, the gratings strength is larger for 0 μm then for 50 μm due to lower average temperature in the displaced position, in spite of the fact that the temperature gradient is higher.

4. Conclusion

We have demonstrated that the origin of antisymmetric perturbation of the fiber in arc-induced long-period gratings that couple the core mode into the antisymmetric LP_{1i} cladding modes is the temperature gradient in the arc discharge. We have shown that this gradient causes a temperature gradient in the fiber, which results in a gradient of viscosity and a corresponding asymmetry of fiber deformation. The effect of microdeformation consisting in periodical core shift is strong enough to produce gratings with coupling strengths as large as measured in experiments. By shifting the fiber to a region with stronger temperature gradient it is possible to increase the reproducibility of the process of the grating inscription for the case of coupling to the antisymmetric cladding modes.

#83839 - $15.00 USD Received 7 Jun 2007; revised 13 Aug 2007; accepted 13 Aug 2007; published 8 Oct 2007